Jurnal Tribologi 31 (2021) 55-72

MYTRIBOS Malaysian Tribology Society

Jurnal Tribologi

Website : jurnaltribologi.mytribos.org e-issn: 2289-7232

Effect of PVD process parameters on TiAlN coated cutting tool flank wear performance

Md Nizam Abd Rahman [1*], Mohamad Ridzuan Jamli [1], Mohd Nazim Abdul Rahman [2], Rohana Abdullah [3], Bobby Umroh [4], Mohd Amri Sulaiman [1]

[1] Fakulti Kejuruteraan Pembuatan, Universiti Teknikal Malaysia Melaka, MALAYSIA.
[2] Fakulti Kejuruteraan Mekanikal, Universiti Teknikal Malaysia Melaka, MALAYSIA.
[3] Fakulti Teknologi Kejuruteraan Mekanikal dan Pembuatan, Universiti Teknikal Malaysia Melaka, MALAYSIA.
[4] Department of Mechanical Engineering, Faculty of Engineering, Universitas Medan Area, INDONESIA.
*Corresponding author: mdnizam@utem.edu.my

KEYWORDS

Physical vapour deposition
TiAlN coating
Flank wear
Single point turning

ABSTRACT

This study focused on the influence of Physical Vapour Deposition (PVD) parameters on the flank-wear of the deposited TiAlN thin-film coating. Response Surface Methodology (RSM) has been selected as the approach of this study. The coating was sputtered onto a tungsten carbide cutting tool insert. A single point turning was performed on the D2 steel to evaluate its flank-wear performance. Also measured are the hardness, grain size, and roughness of the synthesized TiAlN coating using nano-indentor, XRD, and AFM. The result indicated that the quadratic term of bias voltage and the interaction between the substrate temperature and sputter power significantly determined the performance of the coated tool. The quadratic term of the bias voltage is the most influential factor, contributes about 17.25% and the interaction between the substrate temperature and sputter power contributes 9.11% of the effect on the flank wear performance. A polynomial model was developed to model the interrelation between the coating process parameters and the flank-wear. The adequacy of the model is reflected by the strong model correlation coefficient (R^2) of 0.8 and the signal to noise ratio (Adeq. Precision) of 5.773.

Received 2 June 2021; received in revised form 24 Sept 2021; accepted 12 November 2021.
To cite this article: Abd Rahman et al. (2021). Effect of PVD process parameters on TiAlN coated cutting tool flank wear performance. Jurnal Tribologi 31, pp.55-72.

1.0 INTRODUCTION

Hard turning technology is a significantly important manufacturing process that supports the growth of high precision industry, high hardness components manufacturing needs. One of the common materials for such components is AISI D2 steel. Its popularity is due to its superior wear resistance performance compared to some other materials for applications such as forming and thread rolling dies (Kumari et. al., 2018). Hence, it is imperative to be able to select and characterize suitable cutting tools to machine such hard materials.

One of the methods to minimize tool wear during the hard turning process is the application of thin-film hard coating onto the surface of a cutting tool. The hard coating improves the surface characteristics of a workpiece while preserving its bulk properties. There are numerous reports on the cutting tool's live improvement due to the application of hard coating (Sulaiman et. al., 2021; You et. al., 2021). Wang et. al. (2021) reported that the coated tool outlasts the uncoated tool by a huge margin.

Deposition of hard coating onto tool surface could make possible the adoption of minimum quantity lubrication method or even machining without the usage of lubrication. These methods can result in a reduction in manufacturing cost by as much as 15% which can be attributed to the cost of cutting fluid and its disposal (Khan et. al., 2021).

The sputtering process in PVD transfers the target material onto the substrate through the bombardment of target materials by energetic projectile particles such as Argon ions. Upon the bombardment, the target particles were ejected and deposited themselves onto the surrounding surface including the substrate surface (Baptista et. al., 2018). The optimization of the coating process requires a comprehensive knowledge of the process parameters that dictate the quality of the deposited coating. Some reported work on coating process characterization suggested that bias voltage, substrate temperature, and sputter power significantly affecting the coating characteristics (Bobzin, 2017). However, the holistic study of those parameters and the interaction among them is lacking.

There are various design of experiment (DOE) methods that can be used for process characterization such as full-factorial, partial factorial, Taguchi method, and response surface methodology (RSM) methods. RSM and Taguchi methods have been widely used methods in investigating and modeling tool wear performances (Santhanakrishnan et. al., 2021; Shozib et. al., 2021; Horng et. al., 2008, Ayyıldız et. al., 2021; Kara, 2018).

Hence, this study aims to investigate the influence of PVD process parameters on the deposited TiAlN coating flank-wear performance using the RSM approach. The RSM will also enable the identification of significant interactions among the PVD process parameters that affect the flank-wear performance.

2.0 EXPERIMENTAL PROCEDURE

The PVD coating was performed using a VACTEC VTC 1000 coating machine. The target materials are Ti-Al alloy (50 % Ti: 50 % Al) which are vertically mounted on an unbalanced magnetron system. The substrates to be coated are a cutting tool insert (Sumitomo SPGN120308S) made of tungsten carbide (WC) which are mounted on a rotating substrate holder.

The TiAlN coatings were reactively deposited onto the WC substrate with the nitrogen gas as the process gas. The ionized argon gas was utilized to sputter the target material. Before the deposition of TiAlN coating, the WC substrates were treated in an alcohol bath for 20 minutes using an ultrasonic cleaning machine. The gap between the substrate and target when loaded in

the substrate holder is 5 cm and the rotational speed of the substrate holder is five 5 revolutions per minute.

There are three phases in the coating process; substrate cleaning using argon ions bombardment, TiAl interlayer coating (minimize the thermal expansion coefficient differential WC and TiAlN coating, and TiAlN coating deposition. The base coating chamber pressure prior to the start of the coating process was 5.0 x 10^{-5} mbar. Table 1 shows the specific parameter settings for the three phases of the coating experimental run.

RSM (center cubic design) approach was utilized to develop the experimental plan using Design-Expert version 7.0.3. All the statistical analysis was also performed using the same software. The factorial levels were determined based on assigning the axial points (+/- Alpha values) as shown in Table 2 to reflect the extreme operating window of the process parameters.

Table 3 shows the experimental runs for this study. To ensure randomization of the experimental runs, the sequence of the experimental runs was randomized by the software. Three cutting tool inserts were coated per experimental run and the data collected were the average of the three samples. The factorial levels for all parameters were determined based on axial points. That is the reason for some of the settings are in decimal points.

Table 1: The three phases of the coating process.

Substrate ion cleaning	**TiAl Interlayer coating**	**TiAlN deposition**
Argon pressure :	Aron gas pressure:	Ar gas pressure:
5.5 x 10^{-3} mbar	*4.0 x 10^{-3} mbar*	*4.0x 10^{-3} mbar*
Ion source power:	Duration:	Nitrogen gas pressure:
0.24 kV/ 0.4 A	*5 minutes*	*0.4 x 10^{-3} mbar*
Substrate bias:	Other settings:	Duration:
-200V	*similar to the TiAlN*	*90 minutes*
Duration:	*deposition parameter s*	Other settings:
30 minutes		*based on experimental matrix*

Table 2: Axial points for respective process parameters.

	Substrate temperature (°C)	**Substrate bias voltage (V)**	**Sputter power (kW)**
- Alpha	200	50	4
+ Alpha	600	300	8

The measurement of coating tool wear performance was done by measuring the maximum flank-wear of the coated tool insert after the turning process under dry conditions. The measurement was done in accordance with the ISO tool-life testing standard (3685:1993(E)). The turning machining process was conducted using the GATE-Precision (G-410-TCV) lathe machine. AISI D2 steel was selected as the workpiece; the dimensions of the workpiece were 100 mm and 250 mm respectively for the diameter and length. Table 4 shows the material composition specification of the workpiece.

For each experimental run, the TiAlN coated cutting tool was to remove an equal amount of workpiece volume under similar turning process parameters as indicated in Table 5. The single point turning parameter settings in Table 5 is in accordance with tool-life ISO testing standard

(3685:1993(E)), where cutting speed, feed rate, and depth of cut are determined based on tool insert with 0.8 mm corner radius.

Table 3: PVD coating experimental runs based on RSM CCD approach.

Run	A: Sputter Power (kW)	B: Substrate Bias Voltage (V)	C: Substrate Temperature (°C)
1	6	50	400
2	4.81	100.67	518.92
3	4.81	249.33	281.08
4	6	175	400
5	6	175	200
6	4.81	100.67	281.08
7	7.19	249.33	281.08
8	6	175	400
9	6	175	400
10	4.81	249.33	518.92
11	7.19	100.67	281.08
12	6	175	600
13	7.19	249.33	518.92
14	6	175	400
15	8	175	400
16	6	300	400
17	7.19	100.67	518.92
18	4	175	400
19	6	175	400
20	6	175	400

Table 4: AISI D2 steel chemical composition.

Elements	C	Cr	V	Mo	Mn	Si
Composition (%)	1.55	12.0	1.0	0.7	0.3	0.3

The measurement of the flank-wear was done utilizing Zeiss Axiomat 2 optical microscope with software measurement system (version 4.2 Aziovision). The average maximum flank wear of 3 samples was obtained for each experimental run as the output response of the experimental run.

Additional data collected for this study were the thin film micrograph using SEM, grain size using XRD, coating surface morphology and roughness using AFM, and coating hardness using nano-indentation and the setting for respective analysis is as shown in Table 6.

Table 5: Turning parameters based on ISO tool-life testing standard.

Cutting Length (L_c) (m)	**Cutting Speed (V_c) (m/min)**	**Feed rate (f) (mm/rev)**	**Depth of cut (a_p) (mm)**
18	200	0.25	1.6

Table 6: Settings for AFM, XRD, and nano-indentation analysis.

AFM (Shimadzu SPM-9500J2)	**XRD (Bruker D-8 XRD)**	**Nano-indentation (NanoTest)**
The detection mode: *Si3N4 cantilever* Scanning area: *5x 5 microns (25 µm²).*	The analysis conditions: *CuKα radiation, λ = 0.15406 nm, Ni filter, 40 kV and 40 mA* Grazing incidence angle: *1 degree* 2θ scanning range: *30 to 60°, step size of 0.020°, dwell time 1 second* The grain size (Dp): *Scherrer's equation Dp = 0.9 λ/ β2θcosθ*	Indenter: *Berkovitch* Maximum load: *50mN* Dwell time at maximum load: *10 seconds.*

3.0 RESULTS AND DISCUSSION

The typical sample of flank wear images taken using an optical microscope and SEM is shown in Figure 1 and the SEM image of the developed coating layer is shown in Figure 2.

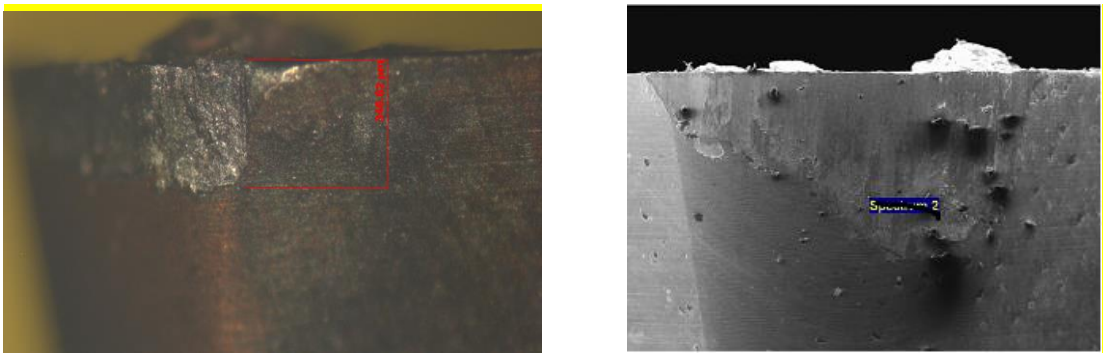

(a) (b)

Figure 1: Typical flank wear image of cutting tool using (a) an optical microscope and (b) SEM.

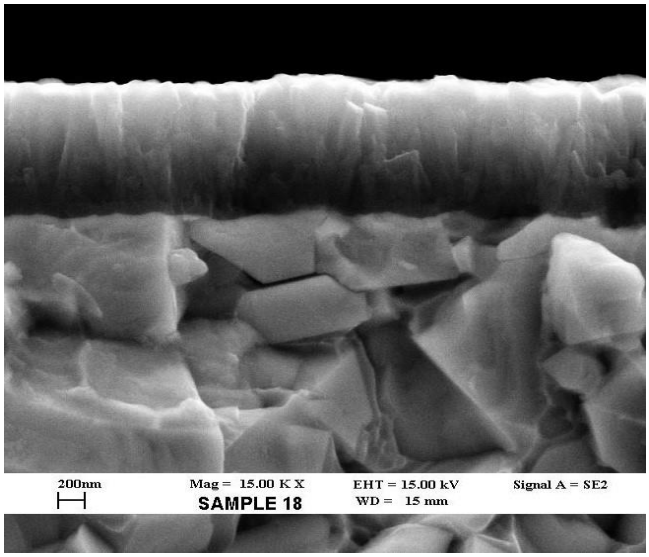

Figure 2: SEM image of the deposited TiAlN coating for the experimental run 18.

The resultant maximum flank wear values for the experimental runs are tabulated in Table 7 and the data were analyzed utilizing Design Expert (version 7.0.3).

The sequential model sum of squares (SMSS) and the lack-of-fit analysis (Table 8 and Table 9) suggested that the quadratic polynomial model is the best to define the interrelation between the flank wear and evaluated PVD process parameters. This is indicated the lowest p-value of SMSS analysis of 0.1024. The cubic model p-value is less than the p-value of the quadratic model, but the cubic model is aliased (the experimental data is inadequate for estimating all the terms) as indicated in the lack-of-fit analysis in Table 9.

The ANOVA of the experimental data (Table 10) indicated that the developed model is representing PVD process parameters and flank-wear relationship at a 90% Confidence Level. The analysis indicates that there is only a 6.5% probability that the "F-value" (2.84) was caused by noise factors. The F-value for lack-of-fit is 2.79, which supported the validity of the model; there is only a 14.51% probability that the Lack-of-Fit (LOF) value was due to chances. The analysis in Table 10 also indicated that the LOF F-value of 2.79 supports the validity of the model where there is a 14.51% chance that a LOF F-value could be due to chances.

Table 7: Experimental matrix and result.

Run	A: Sputter Power (kW)	B: Bias Voltage (Volts)	C: Substrate Temperature (°C)	Flank wear (mm)
1	6	50	400	2.29
2	4.81	100.67	518.92	1.08
3	4.81	249.33	281.08	0.73
4	6	175	400	1.40
5	6	175	200	0.94
6	4.81	100.67	281.08	2.01
7	7.19	249.33	281.08	1.92
8	6	175	400	0.57
9	6	175	400	1.26
10	4.81	249.33	518.92	1.97
11	7.19	100.67	281.08	1.18
12	6	175	600	1.72
13	7.19	249.33	518.92	0.35
14	6	175	400	0.86
15	8	175	400	0.27
16	6	300	400	1.03
17	7.19	100.67	518.92	0.93
18	4	175	400	0.56
19	6	175	400	0.85
20	6	175	400	0.83

Table 8: SMSS analysis for the flank wear model.

Source	Sum of Squares	df	Mean Square	F Value	p-value Prob > F	
Mean vs Total	25.87	1	25.87			Suggested
Linear vs Mean	0.67	3	0.22	0.63	0.6078	
2FI vs Linear	0.7	3	0.23	0.6	0.6247	
Quadratic vs 2FI	1.94	3	0.65	2.11	0.1624	Suggested
Cubic vs Quadratic	2.54	4	0.63	7.27	0.0175	Aliased
Quartic vs Cubic	0.05	1	0.05	0.53	0.5012	Aliased
Fifth vs Quartic	0	0				Aliased
Sixth vs Fifth	0	0				Aliased
Residual	0.47	5	0.095			
Total	32.24	20	1.61			

Table 9: Lack of fit analysis for flank-wear model

Lack of Fit Tests						
Source	**Sum of Squares**	**df**	**Mean Square**	**F Value**	**p-value Prob > F**	
Linear	5.22	11	0.47	5.01	0.0441	
2FI	4.53	8	0.57	5.97	0.0324	
Quadratic	2.59	5	0.52	5.46	0.043	Suggested
Cubic	0.05	1	0.05	0.53	0.5012	Aliased
Quartic	0	0				Aliased
Fifth	0	0				Aliased
Sixth	0	0				Aliased
Pure Error	0.47	5	0.095			

ANOVA analysis can determine the significance of the evaluated parameters as reported by work done by Kara et. al. (2020), Öztürk and Kara (2020), and Kara et. al (2019). The ANOVA table shows the F values and the percentage contribution with the significance level (p-value) of each variable. The F values, as the factors having the most influence on the results, were compared to determine the effect of the evaluated parameters. Based on the ANOVA analysis in Table 10, two sources are considered to be significant in influencing the flank-wear performance. They are the quadratic term of the bias voltage and the substrate temperature and the sputter power interaction. This determination is made by referring to the p-value of those two sources. A P-value of less than 0.1, indicates that there are less than 10% chances that the effects of these two sources on the flank-wear were due to chances. Between those two sources, the quadratic term of the bias voltage is more influential with a 17.25% contribution towards the flank ware; while the substrate temperature and the sputter power interaction contribution is at 9.11%. Also shown in Table 10, the p-value for ABC interaction is less than 0.1, however, the data is inadequate to ascertain its significance because the cubic term (interaction among the three parameters) is considered to be an alias term.

The summary statistics of the flank wear model is shown in Table 10. The coefficient of determination, R^2, value is 0.8. The value of R^2 in the range of 0.7 to 0.89 indicates a strong correlation as reported by Schober et. al. (2018). This indicates that the developed mathematical model can adequately predict the relationship between the evaluated process parameters and the flank wear. Also, from the model statistics in Table 10, the adequate-precision value, that measures the signal-to-noise ratio, is 5.773. A ratio greater than 4 indicates that the model can be used to navigate the design space.

Table10: The ANOVA and model statistics for the flank wear performance

Source	Sum of Squares	df	% Contribution	Mean Square	F Value	p-value Prob > F	Comments
Model	4.83	10		0.48	2.84	0.06	Significant
A-Sputter Power	0.26	1	4.15	0.26	1.53	0.24	
B-Bias Voltage	0.41	1	6.55	0.41	2.38	0.15	
C-Substrate Temperature	2.99E-03	1	0.05	2.99E-03	0.018	0.89	
AB	0.037	1	0.59	0.037	0.22	0.65	
AC	**0.57**	**1**	**9.11**	**0.57**	**3.34**	**0.10**	**Significant**
BC	0.091	1	1.45	0.091	0.53	0.48	
A2	0.4	1	6.36	0.4	2.35	0.16	
B2	**1.08**	**1**	**17.25**	**1.08**	**6.32**	**0.03**	**Significant**
C2	0.35	1	5.59	0.35	2.08	0.18	
ABC	1.53	1	24.44	1.53	8.98	0.015	Alias
Residual	1.53	9	24.44	0.17			
Lack of Fit	1.06	4		0.26	2.79	0.1451	
Pure Error	0.47	5		0.095			
Cor Total	6.37	19					
			Model statistics				
Std. Dev. :	0.4129		**R^2 :**	0.7589		**Adeq. Precision :**	5.7730

3.1 Impact of The Quadratic Term of Bias Voltage on Flank Wear

Figure 3 illustrates the quadratic interrelation between the flank-wear and the bias voltage at constant sputter power (6kW) and substrate temperature (400°C). The increase of substrate bias (50 V to 175 V) resulted in a significant reduction in the flank-wear (2.29 mm to 0.85 mm). However, as the bias voltage is further increased (from 175 V to 300 V) slight increment of flank wear (0.85mm to 1.03 mm) is observed. There is a lack of reporting on this quadratic nature of the interrelation between the bias voltage and flank wear in previous studies. However, Weber et al. (2004) observed that increment of bias voltage (30 V to 125 V) resulted in a reduction in tool wear. There is also contradicting reporting by Ahlgren and Blomqvist (2005) who reported the reduction of coated cutting tool service life with the increment of bias voltage above 100 V. Piecing these two studies together, they explain the finding in this study which indicates the wear performance increases with the increment of bias voltage; however, this trend was reversed slightly when the bias voltage was further raised to 300 V level.

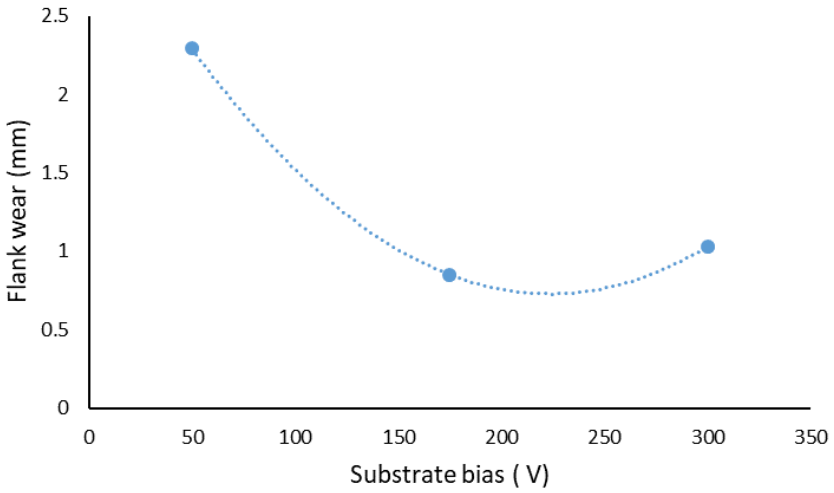

Figure 3: Quadratic relationship between substrate bias and flank wear.

Table 11: Hardness, roughness, and grain size of the TiAlN at various levels of substrate bias voltages.

Run	Bias voltage (V)	Coating Hardness (GPa)	Coating Roughness (nm)	Flank-wear (mm)	Grain size (nm)
1	50	3.54	81	2.29	59.3
19	175	11.27	45	0.85	12.31
16	300	14.14	100	1.03	10.66

Additional data collected to explain the impact of bias voltage variation, while holding the substrate temperature at 600°C and the sputter power fixed at 6kW on the flank wear is tabulated in Table 11. The data correspond to experimental run numbers 1, 19, and 16 as indicated in Table 9. The roughness data were obtained using AFM, the grain size is determined based on XRD data and calculated using the Scherrer formula, and the hardness measurement is obtained from the nano-indentation test.

Figure 4 illustrates the AFM image of the surface of the TiAlN coating for various substrate bias voltages; also, embedded in Figure 4 are SEM images of the fractured cross-section of the TiAlN coating. As the bias voltage increases (50 V to 175 V), the AFM images (Figure 4) indicate the visual smoother surface morphology and reduction of the size of the TiAlN grain. A significant reduction in grain size from 59.3 to 12.31 nm was also observed from XRD data shown in Table 11. The higher coating hardness at high bias voltage can be attributed to the increase in the energy of ion bombardment on the deposited coating. This increased the density of the coating nucleation and refined the coating grain size (Skordaris et. al., 2018). The increase in energy imparting on the developing TiAlN could also anneal out defects on the surface of the TiAlN coating resulting in smoother surface morphology.

The increment of bias voltage from 175V to 300V increases the coating roughness significantly from 45nm to 100nm. The grain size further reduces slightly from 12.31 nm to 10.66 nm. Visually, this is evident from the AFM image in Figure 4(c); even though visually, the grain size

between Figure 4(b) and 4(c) are slightly different, there are imperfections or damage on the surface of the TiAlN film causing the roughness value to increase significantly. This can be attributed to excessive ion bombardment energy levels where the benefits of ion bombardment cannot overcome the detrimental effect it caused (Bouzakis et. al., 2007).

The finer grain size resulted from the increase in coating hardness as shown in Table 9. Corresponding to the finer grain size, the hardness value improves significantly from 3.54 GPa to 11.25 GPa as the function of the bias voltage increment (from 50V to 175V); however, the increment of the hardness is at a much lesser rate as the bias voltage was further increased to 300 V.

Flank wear is proportional to the hardness and inversely proportional to the surface roughness. Surface roughness could impact the material pick-up behavior and friction level of the tool surface as it slides relative to the workpiece material (Lee et. al., 2019; Podgornik et al. 2004). This is aligned with the result in Table 11, which indicates the interrelation between flank-wear with hardness and surface roughness as the bias voltage increases from 50 to 175V. However, as the voltage is further increased to 300 V, the slight increase in hardness cannot overcome the effect of the significant increase in roughness; this resulted in a slight increase in flank-wear within this voltage range.

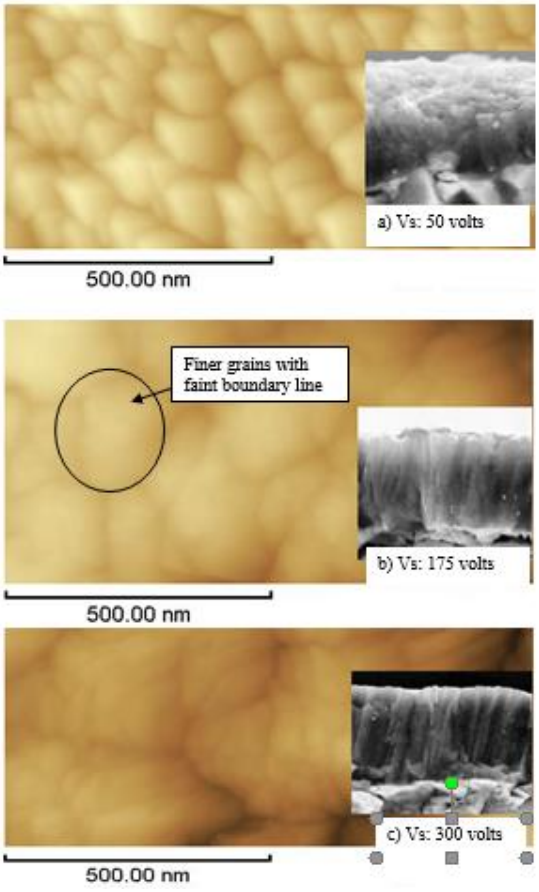

Figure 4: AFM image of TiAlN coating for various substrate bias voltage (Vs).

3.2 Impact of Sputter Power and Substrate Temperature Interaction

Based on the ANOVA analysis in Table 10, the other significant factor that significantly impacting the TiAlN coated tool insert wear performance is the sputter power and substrate temperature interaction. As indicated in Figure 5, the flank-wear increases (0.85 mm to 1.1 mm as sputter power increases (4.8 kW to 7.2kW) while the substrate temperature is fixed at a low level (281°C). However, at a high temperature (519 °C), this trend reversed; the tool wear improves (1.34 mm to 0.53 mm) with the increment in the sputter power (4.8kW to 7.2 kW).

Additional data collected to explain the impact of the sputter power and substrate temperature interaction on flank wear is tabulated in Table 12. The data is corresponding to experimental run numbers 2, 6, 11, and 17.

AFM images in Figure 6 and data in Table 12 indicate that at high substrate temperate (518° C) the surface morphology becomes slightly smoother, and the roughness reading reduces slightly (67.7nm to 65.6nm) as the sputter power decreases indicating the insignificant effect of sputter power at high substrate temperature (518 °C).

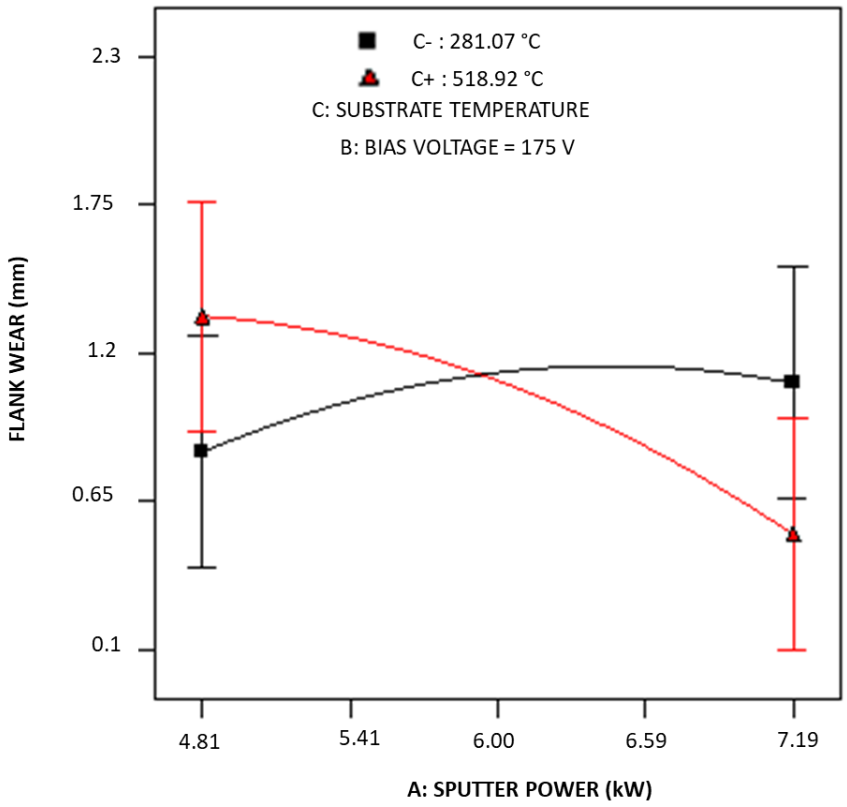

Figure 5: Sputter power and substrate interaction influencing TiAlN coated insert flank-wear.

Table 12: Hardness, roughness, grain size, and flank-wear data for the substrate temperature and sputter power interaction effect.

Run	Substrate Temperature (C)	Sputter Power (kW)	Coating Hardness (GPa)	Coating Roughness (nm)	Grain size (nm)	Flank- wear (mm)
2	518	4.8	5.27	65.60	38.83	1.08
6	281	4.8	4.33	75.60	41.19	2.01
11	281	7	9.76	49.90	14.78	1.18
17	518	7	8.88	67.30	14.88	0.93

This can be attributed to the suppression of crystalline preferential growth at elevated temperature which resulted in a smooth surface without being influenced by the level of sputter power (Lugscheider et al. 1996). This is reflected by the AFM images in Figure 6(Run 2 and Run 17) that show the TiAlN surface morphology with high substrate temperature (518 °C) has a globular and smooth surface morphology. At lower temperature (218 °C), the surface morphology is more jagged (Run 6 and Run 11).

The synthesized coating surface roughness and surface morphology, as indicated in Figure 6 and Table 12, are greatly influenced by the change of sputter power when the substrate temperature is fixed at 281°C. The increase in sputter power (4.8kW to 7kW) at low temperature (281°C) reduces the surface morphology and surface roughness (75.60 nm to 49.90nm). The low-temperature and high sputter power conditions increase the sputter rate and the nucleation rate and at the same time limit the self-shadowing occurrence. The self–shadowing effect limits the accumulation of atomized coating atoms or ions at the specific area of the substrate due to oblique deposition of the coating particles. This will result in coating with rougher surface morphology. Reduction in self-shadowing effect at low-temperature and high sputter power increase the probability of particle accumulation on the substrate surface of different deposition angles which resulting in smoother morphology and lower roughness (Mattox, 2010; Wuhrer and Yeung, 2004).

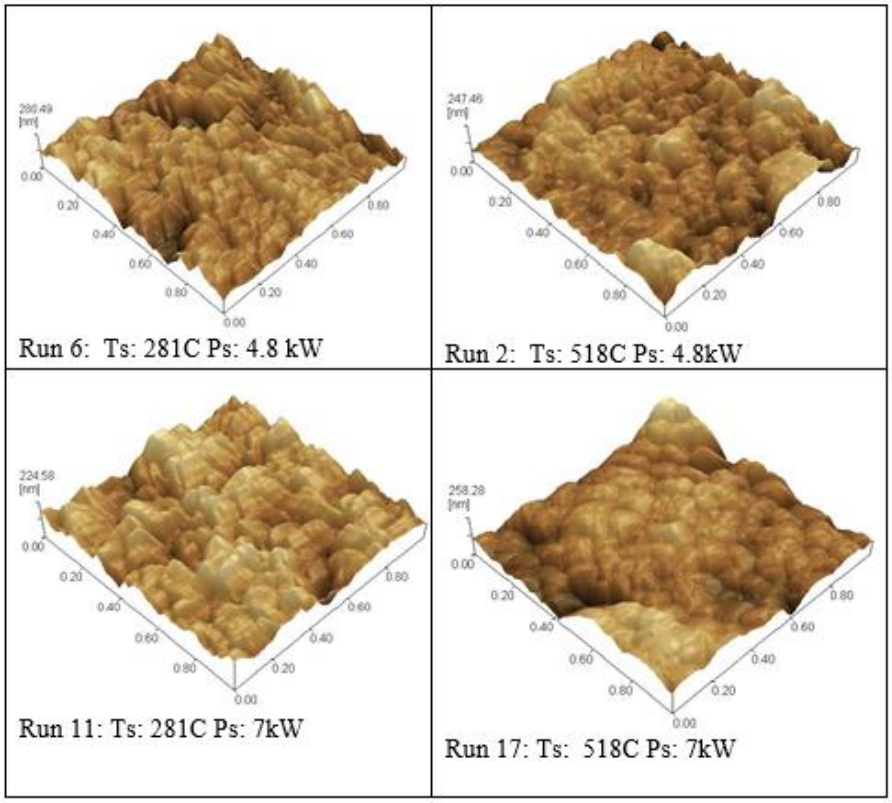

Figure 6: Effect of substrate temperature and sputter power interaction on coating surface.morphology.

The hardness of the TiAlN coated tool insert is greatly affected by the sputter power as shown in Table 12 where the low sputter power (4.8kW) resulted in lower hardness (4.33- 5.27 GPa) compared to the higher sputter power (7kW) which resulted in higher hardness (8.88- 8.76 GPa). This can be ascribed to the finer grain size range (14.78nm to14.88 nm) formation for the higher sputter power compared to grain size range (38.83nm - 41.19 nm) at lower sputter power (4.8kW).

3.3 Polynomial Equation Model of Tool Wear Performance

Table 13 shows the coefficient estimate that represents the expected change in response per unit change in factor when all remaining factors are held constant. The intercept in an orthogonal design is the overall average response of all the runs. The Variance Inflation Factor (VIF) is a measure of the amount of multicollinearity in a set of multiple regression variables. The acceptable value of VIF is less than 5 (James et.al., 2017). As shown in Table 13, the VIFs for all the factors are within the range of 1 to 1.02, indicating that the coefficient estimates for all the factors are acceptable.

Table 13: Coefficient estimate in terms of actual factors.

Factor	Coefficient Estimate	df	Standard Error	VIF
Intercept	+15.72843	1	0.1684	
A-Sputter Power	-0.99562	1	0.1117	1.0000
B-Bias Voltage	-0.12889	1	0.1117	1.0000
C-Substrate Temperature	-0.043465	1	0.1117	1.0000
AB	0.017406	1	0.1460	1.0000
AC	$+5.3952 \times 10^{-3}$	1	0.1460	1.0000
BC	$+ 2.6164 \times 10^{-4}$	1	0.1460	1.0000
A^2	-0.11774	1	0.1088	1.02
B^2	$+4.9474 \times 10^{-3}$	1	0.1088	1.02
C^2	$+ 1.1076 \times 10^{-5}$	1	0.1088	1.02
ABC	-4.1599×10^{-5}	1	0.1460	1.000

Base on the coefficient estimate for the factors in Table 13, the behavior of flank-ware performance relatives to the variation of coating process parameters (bias voltage, sputter power, and substrate temperature) can be represented by the equation below.

$$\textit{Flank wear} = 15.75645 - 0.99562 \times Sp - 0.12889 \times Vs - 0.043465 \times St + 0.017406 \times Sp \times V + 5.3952 \times 10^{-3} \times Sp \times St + 2.6164 \times 10^{-4}\, Vs \times St - 0.11774 \times Sp^{2} + 4.9474 \times 10^{-3}\, Vs^{2} + 1.1076 \times 10^{-5}\, St^{2} - 4.1599 \times 10^{-5} \times Sp \times Vs \times St$$

Where,

Sp : Sputter Power in kW
St : Substrate temperature in °C
Vs : Substrate bias voltage in V

Graphically, the model can be represented by the graph in Figure 7, at a constant substrate bias voltage of 175V. The developed model can only be used to predict the behavior of the PVD process within the range of the factorial limit of the experiment only (Sputter Power: 4.8- 7.2 kW; Substrate temperature: 281- 518 °C; Substrate bias voltage: 100- 250 V).

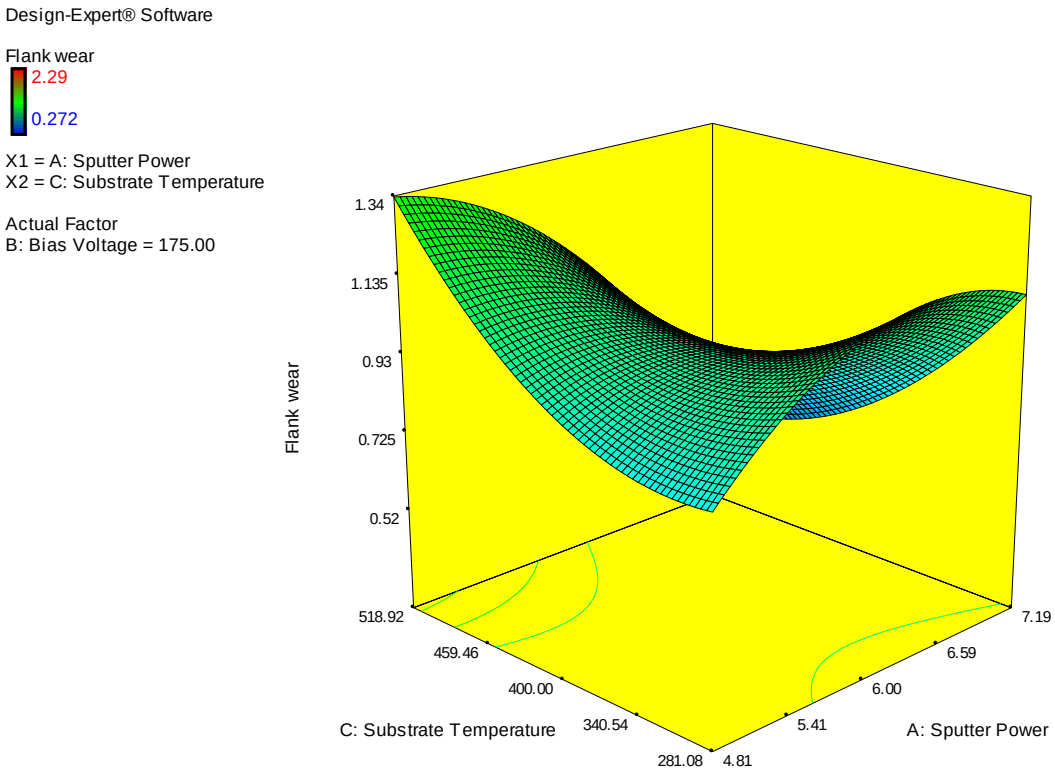

Figure 7: Flank wear response surface model at a fixed bias voltage of 175 V.

CONCLUSIONS

The finding from this study indicated that the quadratic term of bias voltage and the interaction between the substrate temperature and sputter power significantly determined the performance of the coated tool with respect to flank-wear. This is based on the Prob >F value of less than 0.1 for both factors. The quadratic term of the bias voltage is the most influential factor, contributes about 17.25% in linear term and the interaction between the substrate temperature and sputter power contributes 9.11% of the over effect on the flank wear performance.

The substrate bias quadratically influences the flank-wear, where initially the increment of bias voltage reduces the flank-wear. However, its influence diminishes beyond 175 volts. There is an indication that the flank-ware gets worse when the bias voltage is increased beyond this level. There is a strong substrate temperature and sputter power interaction when the substrate temperature is set at 218°C. However, at a temperature of 518°C, the reverse is true. The flank-wear reduces with the increment in the sputter power.

A polynomial model was defined to model the relationship between the coating process parameters (sputter power, substrate temperature, and bias voltage) and the flank-wear. The adequacy of the model is reflected by the strong model correlation coefficient (R^2) of 0.8 and the signal to noise ratio (Adeq. Precision) value of 5.773. The developed model can only be used to predict the behavior of the PVD process within the range of the factorial limit of the experiment only. Based on the model, the optimum flank-wear performance can be achieved when operating

at the high substrate temperature of 518 °C, high sputter power of 7kW, and substrate bias at 175V.

ACKNOWLEDGMENT

The authors would like to thank Universiti Teknikal Malaysia Melaka (UTeM) for data and financial support.

REFERENCES

Ahlgren M. and Blomqvist H. (2005). Influence of bias variation on residual stress and texture in TiAlN PVD coatings. Surface & Coatings Technology, 200, 157-160.

Ayyıldız E. A., Ayyıldız M., Kara F. (2021). Optimization of Surface Roughness in Drilling Medium-Density Fiberboard with a Parallel Robot. Advances in Materials Science and Engineering, vol. 2021, Article ID 6658968, 8 pages.

Baptista A., Silva F.J.G., Porteiro J., Míguez J.L., Pinto G., Fernandes L. (2018).On the Physical Vapour Deposition (PVD): Evolution of Magnetron Sputtering Processes for Industrial Applications, Procedia Manufacturing, 17, 746-757.

Bobzin K. (2017). High-performance coatings for cutting tools. CIRP Journal of Manufacturing Science and Technology, 18, 1-9.

Bouzakis K.D., Skordaris G., Michailidis N., Mirisidis I., Erkens G., and Cremer R. (2007) Effect of film ion bombardment during the pvd process on the mechanical properties and cutting performance of TiAlN coated tools. Surface and Coatings Technology, 202 (4–7), 826-830.

Horng J.T., Liu N.M., Chiang K.T. (2008). Investigating the machinability evaluation of Hadfield steel in the hard turning with Al2O3/TiC mixed ceramic tool based on the response surface methodology. Journal of Materials Processing Technology, 208(1–3), 532-541.

James G., Witten D., Hastie T., Tibshirani R.(2017). An Introduction to Statistical Learning: With Applications in R., Springer.

Kara F. (2018). Optimization of Cutting Parameters in Finishing Milling of Hardox 400 Steel. International Journal of Analytical, Experimental and Finite Element Analysis, RAME Publishers, 5(3), 44-49.

Kara F. and Takmaz A. (2019). Optimization of cryogenic treatment effects on the surface roughness of cutting tools. Materials Testing, 61(11),1101-1104.

Kara, F., Köklü U. and Kabasakaloğlu U. (2021). Taguchi optimization of surface roughness in grinding of cryogenically treated AISI 5140 steel. Materials Testing, 62(10), 1041-1047.

Khan T., Broderick M., and Taylor, C.M. (2021). Investigating the industrial impact of hydraulic oil contamination on tool wear during machining and the development of a novel quantification methodology. Int J Adv Manuf Technol, 112, 589–600.

Kumari S., Kumar A., Kumar Yadav R., Vivekananda K. (20180). Optimisation of Machining Parameters using Grey Relation Analysis integrated with Harmony Search for Turning of AISI D2 Steel. Materials Today: Proceedings, 5(5-2), 12750-12756.

Lee W. L., Tokoroyama T., Murashima M., and Umehara N. (2019). Investigating running-in behavior to understand wear behavior of ta-C coating with filtered cathodic vacuum arc deposition. Jurnal Tribologi, 23, 38-47.

Lugscheider E., Barimani C., Wolff C., Guerreiro S., and Doepper G., (1996). Comparison of the structure of PVD-thin films deposited with different deposition energies." Surface & Coatings Technology, 86-87, 177-183

Mattox D.M. (2010). Handbook of Physical Vapor Deposition (PVD) Processing, William Andrew.

Öztürk B., Kara F. (2020). Calculation and Estimation of Surface Roughness and Energy Consumption in Milling of 6061 Alloy. Advances in Materials Science and Engineering, vol. 2020, Article ID 5687951, 12 pages.

Podgornik B., Hogmark S., and Sandberg O. (2004). Influence of surface roughness and coating type on the galling properties of coated forming tool steel. Surface & Coatings Technology, 184, 338-348.

Santhanakrishnan M., Venkateshwaran N., Rajkumar M., Vignesh T. (2021). Performance evaluation of Ni/Nano SiC coated tool insert for machining SS316l using Response Surface Methodology (RSM). Materials Today: Proceedings. 10.1016/j.matpr.2021.04.642.

Schober P., Boer C., Schwart L.A. (2018). Correlation Coefficients: Appropriate Use and Interpretation, Anesthesia & Analgesia, 126(5), 1763-1768.

Shozib I.A., Ahmad A., Rahaman M.SA. , Abdul-Rani A. M., Alam M.A., Beheshti M., Taufiqurrahman I. (2021). Modelling and optimization of microhardness of electroless Ni–P–TiO2 composite coating based on machine learning approaches and RSM. Journal of Materials Research and Technology, 12, 1010-1025.

Skordaris G., Bouzakis K.D., Charalampous P., Kotsanis T., Bouzakis E., Bejjani R. (2018). Bias voltage effect on the mechanical properties, adhesion and milling performance of PVD films on cemented carbide inserts. Wear, 404–405, 50-61.

Sulaiman M. H., Raof N. A., and Dahnel A. N. (2021). The investigation of PVD coating, cryogenic lubrication and ultrasonic vibration on tool wear and surface integrity in manufacturing processes. Jurnal Tribologi, 28, 105-116

Wang Q., Jin Z., Zhao Y., Niu L., and Guo J. (2021) A comparative study on tool life and wear of uncoated and coated cutting tools in turning of tungsten heavy alloys. Wear, 203929.

Weber F.R., Fontaine F., Scheib M., Bock W. (2004). Cathodic arc evaporation of (Ti,Al)N coatings and (Ti,Al)NyTiN multilayer-coatings—correlation between lifetime of coated cutting tools, structural and mechanical film properties. Surface and Coatings Technology 177 –178, 227–232.

Wuhrer R. and Yeung W.Y. (2004). Grain refinement with increasing magnetron discharge power in sputter deposition of nanostructured titanium aluminium nitride coatings. Scripta Materialia, 50, 813-818.

You Q., Xiong J., Guo Z., Huo Y., Liang L., Yang L. (2021). Study on coating performance of CVD coated cermet tools for 4340 steel cutting. International Journal of Refractory Metals and Hard Materials, 98 -105554.